Journal of Applied Polymer Science

Exploring a highly dispersible silica–elastomer composite for tire applications

Partheban Manoharan, Kinsuk Naskar
Rubber Technology Centre, Indian Institute of Technology, Kharagpur, India
Correspondence to: K. Naskar (E-mail: knaskar@rtc.iitkgp.ernet.in)

ABSTRACT: In this article, we provide an extensive analyses of various properties that are required for tire tread based on developed highly dispersible (HD) silica-filled epoxidized natural rubber composites. Silica in an HD form has become a staple filler in tire tread applications because of its inherent advantages. In this study, epoxidized natural rubber with 25 mol % epoxide (ENR 25) and natural rubber were mixed with two different types of HD silica for superior reinforcement. A standard tire tread formulation was used as the base compound. The magic triangle properties were conspicuously influenced by the viscoelastic characteristics of the vulcanizates. The introduction of polar rubber (ENR 25) into the HD silica greatly improved rheological, physicomechanical, bound rubber content, and dynamic mechanical properties, and this led to a better, fuel-efficient tire. We successfully achieved this, even in the absence of a silane coupling agent. ENR 25 played an imperative role in showing an extraordinary rubber–filler interactions and was primarily responsible for these observations. In this study, we explored the HD silica dispersion with transmission electron microscopy observations. Morphological studies revealed well-dispersed HD silica with the formation of a rubber–filler network. © 2016 Wiley Periodicals, Inc. J. Appl. Polym. Sci. **2016**, *133*, 43531.

KEYWORDS: composites; elastomers; mechanical properties; morphology

Received 2 December 2015; accepted 8 February 2016
DOI: 10.1002/app.43531

INTRODUCTION

Silica is preferred as complimentary to carbon black as a reinforcing filler in tire tread compounds.[1] Natural rubbers (NRs) with silica-filled tire treads have become known as green tires because of their significant gain in tire properties.[2] Recently, a new generation of silica called highly dispersible (HD) silica has attracted researchers because of its superior functional properties.[3] Silica has a significant influence on tire tread applications because of its advantage, such as a reduction in the rolling resistance, a high wet grip, a low heat buildup (HBU), and a reduction in the Payne effect ($\Delta E'$).[4] Silica, by virtue of its manufacturing process, is characterized by hydrophilicity because of the presence of silanol groups on the surface. It is incompatible with nonpolar rubbers such as NR.[5] Bifunctional organosilanes such as bis(triethoxysilyl propyl) tetrasulfide (TESPT) are being used as coupling agents to improve compatibility at the nanoscale through the creation of chemical links. The interaction between the filler and rubber occurs through the formation of a chemical linkage through silanization.[6] Epoxidized natural rubber (ENR) is a modified form of NR. Its chemical and physical properties are different from those of NR. ENR is a highly polar rubber because of the epoxide functional groups randomly dispersed along the rubber backbone. ENR interacts with hydroxyl groups on the silica surface because of the polar functional groups present in the structure.[7,8] The silica–rubber interaction is a key parameter in the reinforcement of polar and nonpolar rubber.[9] ENR has been used as a compatibilizer in silica-filled NRs, and the physicomechanical and dynamic mechanical properties were improved. ENR, particularly at a lower concentration [e.g., in epoxidized natural rubber with 25 mol % epoxide (ENR 25)] is able to undergo strain-induced crystallization.[10,11] In addition, the ratio of ENR to unmodified NR has to balance cocurability to sustain a resilience and fatigue life that are superior to those of NR and are largely required in tread applications.[12] In ENR, high degrees of reinforcement are achieved with silica fillers without the requirement of silane; ENR can be activated by the hydroxyl groups on the silica surface.[13,14] TESPTs are the most efficient coupling agents for silica-filled NR composites. It has been reported that the mechanical properties of silica-filled ENR/NR blends without a coupling agent resulted in an excellent set of properties comparable to those of silica-filled NR.[15–17] $\Delta E'$ was significantly reduced by the presence of TESPT in silica-filled composites; this increased the level of reinforcement and filler dispersion. However, the rubber–filler interactions contributed to the strain independence of the modulus. The bound rubber content (BRC) is an indicator of how much filler is associated with rubber bonds. The bound rubber, as a physical

Table I. Compound Formulations and Designations

Ingredient	1Go	1G	1B	1N	2Go	2G	2B	2N
ENR 25 (phr)	100	100	50		100	100	50	-
NR (phr)	-	-	50	100	-	-	50	100
HD silica Zeosil 1085 GR (phr)	60	60	60	60	-	-	-	-
HD silica Zeosil 1165 MP (phr)	-	-	-	-	60	60	60	60
TESPT (phr)	-	2.5	2.5	2.5	-	5.1	5.1	5.1
Calcium stearate (phr)	3	3	3	-	3	3	3	-
ZnO (phr)	4	4	4	4	4	4	4	4
Stearic acid (phr)	2	2	2	2	2	2	2	2
TDAE oil (phr)	10	10	10	10	10	10	10	10
Antioxidant TMQ (phr)	1.5	1.5	1.5	1.5	1.5	1.5	1.5	1.5
DPG (phr)	0.6	0.6	0.6	0.6	1.2	1.2	1.2	1.2
CBS (phr)	1.5	1.5	1.5	1.5	1.5	1.5	1.5	1.5
Sulfur (phr)	2	2	2	2	2	2	2	2

TMQ, polymerized 2,2,4-trimethyl 1,2 dihydroquinoline

phenomenon, has exhibited avenues for the reinforcement of silica-filled compounds.[18–20]

Saramolee *et al.*[21] evaluated the use of epoxidized low-molecular-weight NR with 28 mol % epoxide as a compatibilizer in silica-filled NR compounds. It improved the mechanical properties with a lower amount of TESPT (1.5 phr) and was comparable to those with a higher loading of 4.5 phr TESPT in the NR silica-filled compound. Kaewsakul *et al.*[22] described an optimal loading of the silane coupling agent TESPT in silica-filled NR compounds at approximately 9.0 wt % in proportion to the amount of silica. Gheller *et al.*[23] varied the amount of TESPT up to 10% in a silica-filled NR blend with styrene–butadiene rubber compounds. They concluded that the 10% TESPT had more influence on the dynamic properties of the silica-filled compound. Cataldo[24] reported that the good technological results were obtained by compounding silica with ENR without a silane coupling agent. They proposed that enhanced rubber–filler interaction would be possible through a hydrogen-bonding mechanism between the epoxide groups of ENR and the silanol groups on silica. Dierkes *et al.*[25] studied the various specific cetyltrimethylammonium bromide (CTAB) surface area of silica in a typical tire tread compound. The lower particle size silica showed a higher reinforcement effect and improved mechanical and dynamic properties. Sarkawi *et al.*[26] reported that skim rubber vulcanizates exhibited a higher $\Delta E'$ in a silica-filled compound. This was due to the nondisruption of the silica–silica network by proteins. The microdispersion of a silica-filled compound was evaluated by transmission electron microscopy (TEM), and it was a beneficial tool to achieve a network visualization of rubber–filler interaction. Previously, TEM was used by Chapman and coworkers[13,19,27] to evaluate the dispersion of silica in NR and ENR composites. In the ENR silica-filled composites, no voids were seen, and this indicated high rubber–filler interactions.

In this study, we aimed to analyze the influence of HD silica as a filler in a rubber compound for tire tread applications. The effect of ENR 25 with two different specific surface areas of HD silica in the presence and absence of a coupling agent were investigated for enhanced compatibility between the silica and rubber. We examined the significance to the physicomechanical and dynamic mechanical properties. These studies were validated with TEM, BRC, $\Delta E'$, and so on.

EXPERIMENTAL

Materials

NR [ribbed smoke sheet 3 (RSS 3)] and ENR 25 were supplied by the Malaysian Rubber Board (Malaysia). The reinforcing fillers used in this study were HD silica with CTAB specific surface areas of 160 and 80 m^2/g (trade names Zeosil 1165 MP and Zeosil 1085 GR, respectively) from Solvay Silica (South Korea). TESPT [$(C_2H_5O)_3$—Si—$CH_2)_3$—S_4—$(CH_2)_3$—Si—$(C_2H_5O)_3$] was procured from Evonik. Treated distillate aromatic extract (TDAE) oil, polymerized 2,2,4-trimethyl-1,2-dihydroquinoline, calcium stearate, diphenyl guanidine (DPG), *N*-cyclohexyl-2-benzothiazole sulfenamide (CBS), zinc oxide (ZnO), stearic acid, and sulfur were procured from local companies in India.

Preparation of the Rubber Compound

The silica compounds were prepared with the formulations shown in Table I. The samples were designated as 1Go, 1G, 1B, 1N, 2Go, 2G, 2B, and 2N. The Mooney viscosity [ML(1 + 4) 100 °C] values of RSS 3 and ENR 25 were 88 and 83. 1Go and 2Go refer to the absence of a silane coupling agent in the formulation. The amounts of TESPT and DPG applied in these silica-filled rubber compounds were based on the CTAB specific area of the silica type with the experiential equation proposed by Guy *et al.*[28] The amounts of TESPT and DPG were calculated with the following equations:

$$\text{TESPT(phr)} = 5.3\times10^{-4}\times\text{CTAB specific area of silica}\times[\text{silica(phr)}] \quad (1)$$

$$\text{DPG(phr)} = 1.2\times10^{-4}\times\text{CTAB specific area of silica}\times[\text{silica(phr)}] \quad (2)$$

Table II. Mixing Procedure: Stages I and II

Time (min)	Stage I (master batch): Internal mixer and addition of ingredients
0.00	Add rubber.
1.00	Add other ingredients (ZnO, stearic acid, etc.).
2.00	Add half of silica, silane, and TDAE oil.
4.00	Add second half of silica, silane, and TDAE oil.
6.00	Sweep.
8.00	Dump (~135°C).
Time (min)	Stage II (final batch): Two-roll mill
0.00	Add a master batch compound.
1.00	Add DPG, CBS and sulfur.
4.00	Sheet out.

Kaewsakul *et al.*[22] suggested a two-stage mixing procedure for silica-filled compounds. In stage I, all ingredients, except the curatives CBS, DPG, and sulfur, were mixed in a Haake Rheomix OS (Germany) 600 internal mixer, having a mixing chamber volume of 85 cm^3. All of the mixing was carried out at about 110 °C at a rotor speed of 60 rpm. The mixer fill factor was 70%. Rubber was initially masticated for 1 min. Then, half of the silica was added to silane, TDAE oil, ZnO, stearic acid, and 2,2,4-trimethyl-1,2-dihydroquinoline mixed for 3 min. The remaining amount of silica, silane, and TDAE oil were subsequently added together and mixed for 4 min. The masterbatch compounds were discharged from the internal mixer in clump form and sheeted out on a two-roll mill; we kept a master batch for overnight before incorporation. The dump temperature of the masterbatch compound was approximately 130–135 °C. In stage II, CBS, DPG, and sulfur curative were added to the masterbatch in a Schwabenthan 100-mL, two-roll mill. The detailed mixing procedures are specified in Table II.

Curing Characteristics and Mooney Viscosity

The curing characteristics were measured with a Monsanto model R-100S oscillating disc rheometer according to ASTM D2084. The arc amplitude was at 3° at a temperature of 150 °C for a 30-min period, and we determined the optimum vulcanization time (t_{90}). The sheet obtained from the two-roll mill was then pressed in a compression-molding press (Moore Presses, Birmingham, United Kingdom) to a respective t_{90} at 150 °C under a pressure of 5 MPa. The compounds were tested for their Mooney viscosities with a Negretti Automation Mooney viscometer at a condition ML(1 + 4) 100 °C according to the ASTM D1646. The rate of the curing reaction was determined by curing rate index (CRI), as given by eq. (3):

$$\mathrm{CRI} = 100/(t_{c90} - t_{s2}) \tag{3}$$

where t_{c90} is the curing time and t_{s2} is the scorch time.

Mechanical Characteristics

The tensile and tear properties of the specimen were tested with a Hounsfield H25KS universal testing machine. According to the test methods ASTM D624 and ASTM D412, the specimens were punched from molded sheets 2 mm thick with an ASTM Die-C. A crosshead speed of 500 mm/min was used, and measurements were done at ambient temperature. The hardness of the specimen was carried out in five different places on the specimen with a Shore A durometer hardness tester. The median value was the representative hardness of the certain specimen according to the test method ASTM D2240.

The abrasion characteristics of the specimen were measured with a Wallace Akron abrasion tester in accordance with the test method BS 903. Abrasion loss was expressed in terms of volume loss (cubic millimeters) on the basis of a standard specimen. HBU measurement was determined with a Goodrich flexometer according to ASTM D623 method A. The specimens were conditioned at 50 °C for 30 min before we placed them between the platens. The HBU test was carried out for 25 min, and an increase in the temperature at the base of the specimen was recorded. Then, a temperature rise was determined. The rebound resilience of the rubber specimen was carried out with a Wallace Dunlop tripsometer according to the test method defined by BS 903: Part A8. The dropping angle of the pendulum was 45°, and the rebound angle (θ) was noted directly on the dial. The percentage of rebound resilience was calculated according to eq. (4):

$$\text{Rebound resilience}\,(\%) = (1-\cos\theta)/(1-\cos 45^\circ)\times 100 \tag{4}$$

Characterization of the Filler–Filler and Filler–Rubber Interactions

BRC. The BRC measurements were carried out on unvulcanized samples and samples without curative. An amount of 0.2 g of the sample was put into a metal cage and immersed in 50 mL of toluene for 72 h at room temperature to extract the unbound rubber, and the toluene was renewed for every 24 h. The sample was detached from toluene, dried at 100 °C for 24 h, and weighed. The amount of BRC was calculated with eq. (5):

$$\mathrm{BRC}(\%) = (w_{\mathrm{dry}} - w_s)/w_r \tag{5}$$

where w_{dry} is the dry weight of the specimen after extraction, w_s is the weight fraction of silica in the sample, and w_r is the weight fraction of rubber in the specimen. w_s and w_r were calculated with reference to the compound formulation.

Dynamic Mechanical Characteristics. $\Delta E'$ of the filled, vulcanized rubber specimen was studied with a dynamic mechanical analyzer (PerkinElmer DMA 8000). The strain sweep experiment was performed in tension mode at ambient temperature, and the dynamic strain amplitudes were measured from 0.56 to 100% at a constant frequency of 10 Hz. Dynamic mechanical analysis (DMA) temperature sweep testing was carried out under tension mode from −100 to 100 °C at 0.1% strain, a frequency of 10 Hz, and a 3 °C/min heating rate. The storage modulus (E'), loss modulus, and tanδ were recorded as a function of the temperature. This conformed to the test method ISO 4664-1. The value of tanδ at 60 °C was used to predict the tire rolling resistance.

Morphology of the Composite

Analytical TEM analysis of the vulcanizates was performed with a FEI-TECNAI G2 20S TEM instrument operating at an accelerating voltage of 120 kV. The dispersion of the silica-filled rubber was extensively analyzed with an Analytical TEM instrument.

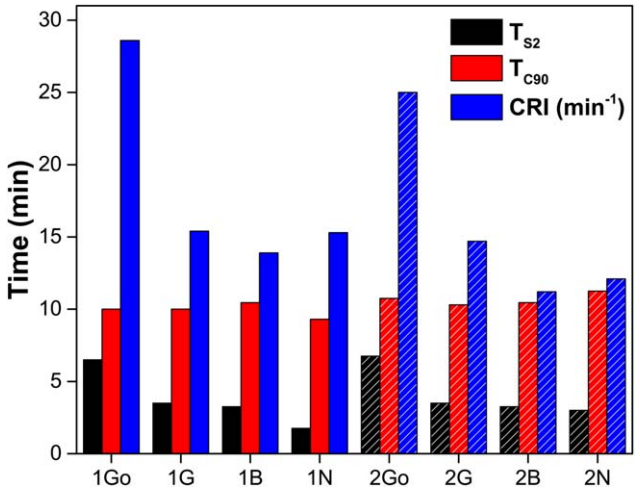

Figure 1. Curing characteristics (t_{s2}, t_{c90}, and CRI) of the HD silica-filled rubber composites. [Color figure can be viewed in the online issue, which is available at wileyonlinelibrary.com.]

The sample preparation for TEM analysis was made by an ultramicrotome with a Leica Ultracut instrument. The ultramicrotome was used below the glass-transition temperature of the blended rubbers ($-70 \pm 5\,^{\circ}C$) with sharpened glass knives with a cutting edge of 45° because of the elastomeric nature of the samples. Digital photomicrographs were captured from cryotomed sections supported on a copper grid.

RESULTS AND DISCUSSION

Curing Characteristics and Mooney Viscosity

Figure 1 shows the t_{s2}, t_{c90}, and CRI. The 1G, 1B, and 1N exhibited lower t_{s2}, t_{c90}, and CRI values compared to the 1Go compound. This was due to the presence of TESPT in the composites. Meanwhile, the mixture of the silica compound with TESPT may have discharged a sulfur donor to the rubber compounds; this may have caused an increase in the crosslinking reactions to ensure that a proper silanization reaction occurred. The silanization reaction often demands optimization, as two out of three ethoxy groups in the triethoxysilyl units of TESPT are converted as ethanol. The incorporation of TESPT leads to strong reductions in the t_{c90} and t_{s2} values of the composites. This behavior was due to the enlargement of the silica–rubber compatibility with the addition of TESPT to the composites. The high-surface-area, silica-filled compounds showed much better curing characteristics compared to the low-surface-area compounds. In the absence of a coupling agent, the 2Go compound also exhibited an equivalent t_{c90}. This adhered to interaction between the epoxide groups and silanol groups on silica. The t_{s2} increase was due to the nonrestriction of the mobility and nondeformability of the ENR matrix with the introduction of mechanical restraints.

The minimum torque (L_i), maximum torque (L_o), and torque difference [ΔL ($L_o - L_i$)] are displayed in Figure 2, respectively. ENR may have formed a monofunctional site link with the silica surface, and it was able to explore a higher curing torque. ENR had polarity differences compared to NR. The polar curatives could easily migrate into ENR because of its polar nature. Moreover, the silanol groups on the silica surface were acidic and caused the adsorption of curatives; this resulted in a delay of the vulcanization reaction and, hence, a reduction in the crosslink density. We were able to delay the vulcanization reaction in the absence of TESPT in the composites 1Go and 2Go. In the presence of TESPT, hydrophobation and lubrication took place into the silica, and this led to a strong reduction in the curing torque. In the presence of silane in ENR, this reduced the degree of adsorption of the polar crosslinking accelerator in the silica surface. As an effect, t_{s2} and T_{c90} decreased. The high-surface-area, silica-filled compound exhibited an overall similar curing torque. ΔL is an indication of the torque established through curing, and it is comparable to the extent of the crosslinking reaction in the compound.[29] The 1Go and 2Go compounds exhibited higher ΔLs. The factor of increases in a CRI based on polarity matches the low filler–filler interaction. However, in this study, the silica-filled compound tended retard curing and provide better scorch safety without the addition of TESPT.

The Mooney viscosity was an important parameter of the compound and was associated with the flow behavior during the processing of a compound. The Mooney viscosities of the silica-filled rubber compounds are listed in Table III. The compound viscosity decreased substantially during the mixing process. During silanization, TESPT present at the surface of silica acted as a slip additive. The viscosities of the silica-filled compounds decreased at the end of the silanization process. In the presence of TESPT, the Mooney viscosities of the silica compounds were effectively reduced. The 1G and 2G compounds displayed sharp decreases in viscosity. As previously discussed for the curing torque characteristics, silica underwent much more hydrophobization, and silanization took place with the epoxide content and alkoxy groups of TESPT through a condensation reaction. The lower viscosity sample exhibited easier processing and obtained a lower energy consumption during processing and better rubber–filler interactions. These results corresponded well with the

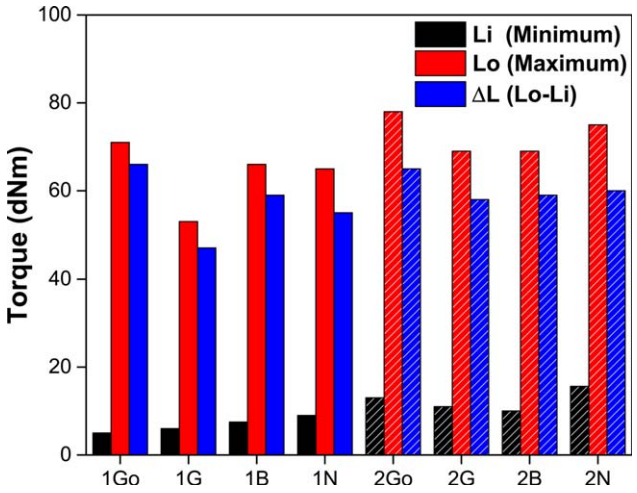

Figure 2. Curing torque characteristics (L_i, L_o, and ΔL) of the HD silica-filled rubber composites. [Color figure can be viewed in the online issue, which is available at wileyonlinelibrary.com.]

Table III. Physicomechanical Properties of the HD Silica-Filled Composites

Properties	Unit	1Go	1G	1B	1N	2Go	2G	2B	2N
Tensile strength	MPa	21 ± 0.7	22 ± 1.8	22.3 ± 0.5	20.4 ± 0.1	24.9 ± 0.2	23.9 ± 0.1	24.5 ± 0.3	24.7 ± 0.2
M_{300}/M_{100}	-	2.8	3.4	3.1	3.0	2.9	3.1	2.9	2.9
Elongation break	%	840 ± 14	720 ± 18	779 ± 8	740 ± 11	820 ± 7	723 ± 6	723 ± 1	679 ± 13
Tear strength	N/mm	51 ± 1.9	45 ± 4.6	86 ± 5.1	107 ± 1.4	87 ± 3.2	73 ± 3.8	109 ± 2.3	113 ± 3.4
Hardness	Shore A	63	66	64	63	69	70	74	76
Abrasion loss	mm^3	22.9 ± 0.9	24.1 ± 0.4	22.2 ± 0.7	18.9 ± 1.2	18.3 ± 0.2	19.5 ± 0.5	17.8 ± 0.5	20.9 ± 0.9
ML(1 + 4) 100°C	MU	40	38	41	43	46	45	49	50
HBU change in temperature	°C	8	8	8	9	8	9	10	9
Rebound resilience	%	43	40	43	40	40	35	40	37

$\Delta E'$ and BRC values. In the absence of TESPT, we obtained a better silica dispersion in the ENR because there were no premature crosslinks in the1Go and 2Go compounds. ENR contained epoxide polar groups and increased the interfacial tension because of the difference between the solubility parameters of ENR and NR. In the case of hydrated silica, some of the water molecules of absorption were loosely termed *silanol groups*. They could open the epoxide link, and we expected the reaction of allylic hydrogens, active for accelerated sulfur crosslinks, to take place. As a result, the polymer could take part in the crosslinking reaction, and we expected to get stronger rubber–filler interaction during the crosslinking and to observe increases in the cure rate and viscosity of the composites.[30]

Physicomechanical Properties of the Vulcanizates

Figure 3 illustrates the tensile stress versus strain plot of the HD silica-filled composites. The tensile strength, elongation at break, and hardness are summarized in Table III. There was no positive influence of the addition of TESPT in the compounds (1G, 1B, 1N, 2G, 2B, and 2N) with respect to the tensile strength. In the absence of TESPT, 1Go and 2Go showed preeminent possible tensile strengths, achieved by the utilization of the epoxide functional group with a silanol group of silica. The higher surface area silica-filled compounds showed much better properties than the low-surface-area, silica-filled compound. This indicated a greater extent of interactions between the silica and rubber phases in the presence and absence of TESPT. To achieve excellent reinforcements in the silica-filled ENR and NR matrixes, the high-surface-area silica easily associated with the epoxide functional groups in ENR because of the lower particle size of the silica. Therefore, the dynamic modulus of the rubber increased with the addition of reinforcing HD silica.

The reinforcement index (i.e., the ratio of moduli M_{300}/M_{100} where M_{300} is modulus at 300% strain and M_{100} is modulus at 100% strain) values are shown in Table III. The reinforcement index is an unconventional measure of the coupling efficiency, as conferred by Rauline.[31] The presence of TESPT compounds showed a higher reinforcement index. It was representative that the silica composite crosslink density increased in the compound. Deagglomeration of the silica in the rubber phase of the compound led a higher modulus at 300%. The elongation break exhibited a significant increase in the absence of TESPT composites (1Go and 2Go). Because of the self-association between the epoxide and silanol groups. The 1N and 2N compounds had higher tear strengths. The tear strength was associated with the crack initiation of the compound. In other compounds containing epoxide groups, the elastic nature of the rubber decreased, and it failed to facilitate a better tear strength in the compound. Therefore, the 1Go and 2Go compounds in the absence of TESPT showed excellent tear strengths compared to 1G and 2G. The hardness values of the 2Go, 2G, 2B, and 2N compounds were subsequently higher than those in the 1Go, 1G, 1B, and 1N compounds. The hardness of the compounds was directly associated with the modulus. These results delivered strong evidence that the mechanical properties were improved in the absence of TESPT.

Abrasion, HBU, and Rebound Resilience

The silica-filled compound exhibited poor properties in abrasion because of the polarity difference between silica and rubber and improper silica dispersion to the rubber phase. In the silica-filled compound, microstructural factors such as the filler morphology, volume fraction, and dispersion of filler were considered better for the abrasion resistance. The high-surface-area,

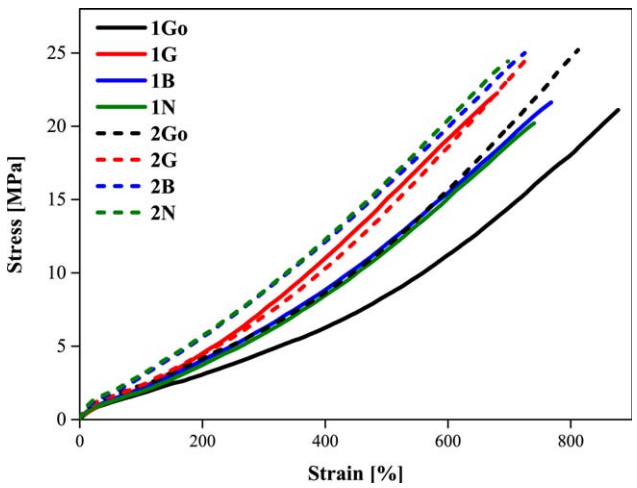

Figure 3. Tensile stress–strain plot of the HD silica-filled rubber composites. [Color figure can be viewed in the online issue, which is available at wileyonlinelibrary.com.]

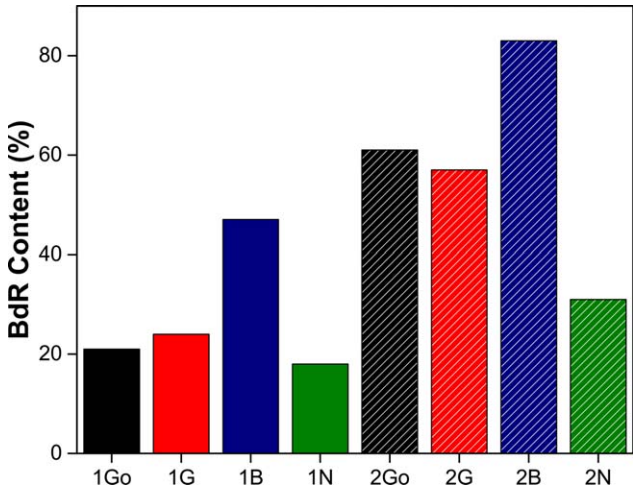

Figure 4. BRC of the HD silica compounds. *BdR*, Bound Rubber. [Color figure can be viewed in the online issue, which is available at wileyonlinelibrary.com.]

silica-filled composite revealed the lowest abrasion loss; this led to better bonding between the rubber–filler networks. Because the presence of TESPT composites (1G and 2G) caused a slightly higher abrasion loss compared to the composites (1Go and 2Go), the abrasion loss primarily depended on the rubber–filler interactions. Therefore, the ENR 25 blend with the NR compound (2B) exhibited a significant decrease in the abrasion loss. The presence of TESPT and epoxide functional groups may have formed better linkages with the silica surface. The fact is that the smaller particle size, silica-filled compound exhibited a lower abrasion loss. During the performance of the tire, a low HBU is essential for fuel efficiency tires. The HBU characteristics of the silica-filled rubber depended on the filler dispersion and crosslink density of the compound. These were the foremost contributors of HBU. Silica-filled compounds imparts significantly poor thermal conductivity. Table III depicts the HBU of silica-filled rubber compounds. However, almost similar values were obtained in the HBU tests, except for the 2B composite. These results corresponded with the dynamic mechanical characteristics of the vulcanizates.

Rebound resilience is directly proportional to the degree of elasticity and segmental mobility. Therefore, the resilience depended on the hardness and stiffness of the compound. ENR 25 was good damping material compared to NR. In 1B, the compound revealed excellent resilience properties obtained by association with ENR and NR compositions. The 2G compound had poor resilience properties in the presence of TESPT. This reduced the elasticity and the mobility segment of the vulcanizates. The 1G, 1N, 2B, and 2N showed more or less equivalent values. In this experiment, the absence of the TESPT compound (2Go) provided excellent resilience and overall better physicomechanical properties.

Influences of Filler–Filler Interactions and Rubber–Filler Interactions of the Silica-Filled Rubber Compounds

The rubber–filler interactions were measured by $\Delta E'$ and BRC. Figure 4 shows the BRC, which was the rubber portion that remained bound to the filler in the uncured compound after it was extracted with toluene. The BRC affected the properties of the silica-filled rubber compounds, such as green strength, viscosity, and curing characteristics. The tightly bound rubber was a primary layer; this was in close contact with a silica particle, and the loosely bound rubber was a secondary layer. It was bound to the primary layer. Connections between the filler and bound rubber were made by two different methods, the direct and indirect methods. The direct method indicated that silica was connected with a primary bound rubber layer or secondary bound rubber layer and was, in an indirect way, connected with a coupling agent. For a normal atmosphere treatment, the rubber chains weakly contact with the secondary layer and are detached from the surface.[32] Hence, the result reveals that direct contact with silica particles and rubber correspondingly brought about better properties in the composites that were comparable to those with the indirect method. This could occur in the epoxide groups with silanol groups through the establishment of strong intermolecular forces through hydrogen bonding. Indirect contact with silica particles through the addition of TESPT led to extraordinary high chemically BRCs formed in the NR and ENR blend matrix. The BRC purely depended on a how rubber chains got connected with the silica surface area, surface activity, and structure. A higher BRC implies higher rubber–filler interactions. In this investigation, the total BRC was carried out in a normal atmosphere. Most of the BRC formed in the 2B compound. On the basis of the results, it was clear that the ENR with TESPT improved the rubber–filler interactions for silica-filled compounds. ENR 25 provided a better compatibility between the high-surface-area silica compounds. The incorporation of ENR in the silica-filled compound caused the formation of strong hydrogen bonds. TESPT was capable of hydrophobizing the HD silica surface and decreased silica agglomeration in the compound. However, in the absence of TESPT, the physical BRC of the 2Go compound indicated a strong interaction with a rubber phase. It was also able to form better linkages with rubber comparable to compounds 2G and 2N. The absorbed silanol groups clearly

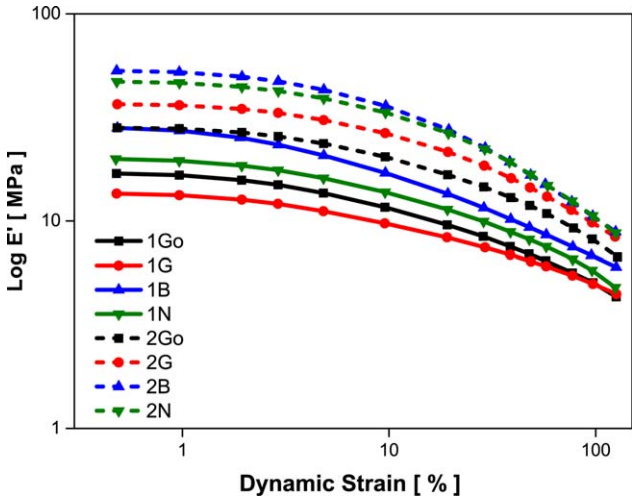

Figure 5. Strain sweep of the HD silica-filled rubber composites. [Color figure can be viewed in the online issue, which is available at wileyonlinelibrary.com.]

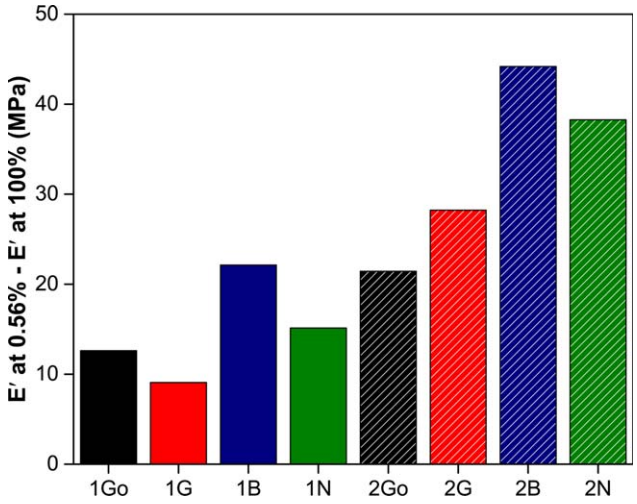

Figure 6. $\Delta E'$ of the HD silica-filled rubber composites. [Color figure can be viewed in the online issue, which is available at wileyonlinelibrary.com.]

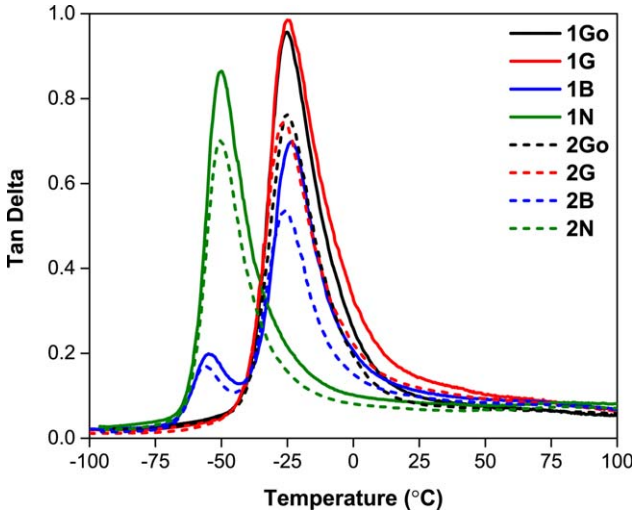

Figure 7. Effect of the HD silica-filled rubber composites on tanδ. [Color figure can be viewed in the online issue, which is available at wileyonlinelibrary.com.]

corresponded well with the epoxide groups by self-association; this led to better rubber–filler interactions without the need for TESPT. The same behavior was observed in the lower surface area, silica-filled compound. In the absence of the coupling agent, the epoxidized rubber chains linked with the silica surface in the manner of a single contact or multicontact on the filler surface; this may have facilitated good rubber–filler interactions. Some of the rubber trapped in the filler aggregates was named occluded rubber. This could be attributed to decrease the mechanical properties.

The degree of filler network formation in the silica-filled compound was characterized by $\Delta E'$. In $\Delta E'$, filler network disruptions took place when the deformations were above a certain amplitude during the strain sweep in DMA and reflected in a decrease in E'. Figure 5 shows the curves of E' versus the dynamic strain amplitude of the silica-filled rubber compound. In the silica-filled compounds, the filler aggregates were in contact to form a continuous filler network in the rubber phase. The presence of the epoxide group or TESPT significantly increasing the rubber–filler interactions. During curing or after mixing, a compound reformation of agglomerates tookplace.[33] The polarity compatibility between rubber–silica prevented agglomerates. E' of the 2Go compound was much lower than those of the other compounds in the high surface area. It was achieved by the absence of TESPT; this was attributed to the good dispersion and strong rubber–filler interaction of the silica in the rubber phase. Figure 6 depicts the $\Delta E'$ values of the HD silica-filled rubber composites. The compounds 2G, 2B, and 2 N in the presence of TESPT exhibited the highest $\Delta E'$; this was an indication of poor dispersion. The low-surface-area-silica-filled compounds 1G,1B, and 1N exhibited the highest $\Delta E'$s in the presence of TESPT. In the presence of epoxide groups and TESPT, this formed additional linkages or interactions, and crosslinks took place with head-to-head molecules and led to a higher $\Delta E'$. The compound with the presence of the coupling agent failed to reach the lowest $\Delta E'$. The 1Go compound revealed a low $\Delta E'$. These results delivered strong evidence that the BRC was improved in the absence of TESPT.

Dynamic Mechanical Characteristics of the Vulcanizates

Figure 7 shows the temperature dependencies of tanδ, and Table IV shows the overall performance of the HD silica-filled compounds predicted by DMA; it was performed at −100 to 100 °C. DMA testing is an investigation of the molecular motion in rubber, and it is an essential method for understanding the performance of tire tread properties. The tanδ values at 60, 10, and −10 °C were shown to be a predictor of the rolling resistance, wet traction, and ice traction of the tread compound, respectively. The tanδ curve at the maximum is often used to identify the glass-transition temperature of a compound with respect to the temperature. The E' values at −20 and 30 °C have

Table IV. Tire Performance of the HD Silica-Filled Rubber Composites Predicted by DMA

Overall performance	1Go	1G	1B	1N	2Go	2G	2B	2N
Winter traction: E' (MPa) at −20°C (lower is better)	80	98	108	48	149	154	146	87
Ice traction: tanδ at −10°C (higher is better)	0.466	0.544	0.340	0.124	0.357	0.355	0.235	0.096
Wet traction: tanδ at 10°C (higher is better)	0.155	0.215	0.145	0.092	0.155	0.119	0.117	0.075
Dry handling: E' (MPa) at 30°C (higher is better)	14	12	21	25	34	29	38	49
Rolling resistance: tanδ at 60°C (lower is better)	0.072	0.096	0.089	0.078	0.066	0.087	0.081	0.068

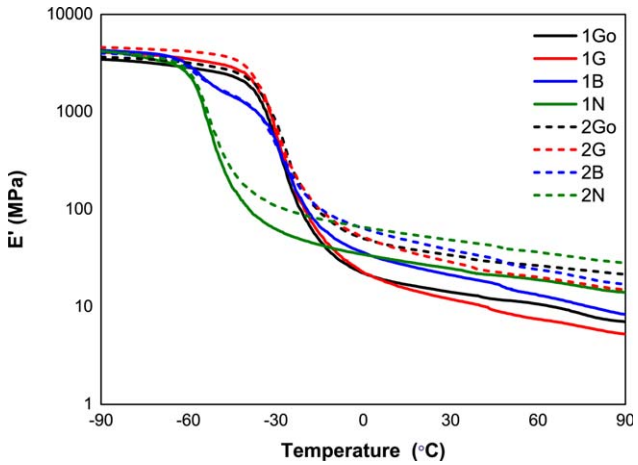

Figure 8. Effect of the HD silica-filled rubber composites on E'. [Color figure can be viewed in the online issue, which is available at wileyonlinelibrary.com.]

been shown to be a predictor of winter traction and dry handling of the compound. It was difficult to obtain the best values of all of the values of tanδ at −10, 10, and 60 °C and E' (−20 and 30 °C).[34] Thus, a balance of these tanδ and E' values suggested an optimum tire tread compound. Many researchers have examined associations between certain viscoelastic characteristics and the tire performances

Figure 8 shows the plot of E' as a function of the temperature. We observed that the E' values of the vulcanizates in the glassy state were in the −90 to −30 °C range. In this temperature range, the 1N and 2N compounds showed significant changes comparable to all of the other compounds (1Go, 1G, 1B, 2Go, 2G, and 2B). The E' values decreased with increasing temperature. The transition from the glassy state to the viscoelastic state occurred at about −30 °C. This was influenced by TESPT bonding with rubber chains to the silica. With these attributes, the 1N and 2N silica-filled compounds with the presence of TESPT exhibited better dry handling and winter traction. The tanδ at 60 °C was an indication of the rolling resistance; the 1Go and 2Go compounds in the absence of TESPT showed a lower tanδ at 60 °C value. This was a sign of fuel efficiency. Therefore, the presence of the TESPT compounds (1G, 1B, 1N, 2G, 2B, and 2N) failed to exhibit a lower tanδ at 60 °C. This was due to the lower chain mobility, and fewer rubber chains were left to contribute to the energy transfer at higher strains and temperatures during dynamic performances. These results were influenced by network contributions to the rubber–filler, and it corresponded well with the tensile modulus. More rubber chains were available to contribute; this, in turn, turn leads to lower energy dissipations at higher strains and temperatures in the 1Go and 2Go compounds. Silica with a lower surface area delivered a higher tanδ peak. The high-surface-area silica reduced the tanδ peak of the increasing rubber–filler interactions. This was observed when we replaced a low-surface-area-silica-filled compound with a higher surface area silica-filled compounds. These were the results of the reduction of the filler–filler network, as confirmed by the $\Delta E'$ results. The 2Go and 1G compounds showed higher tanδ values at −10 °C; this provided better ice traction. The 2Go compound positively influenced the ice traction and rolling resistance but negatively affected the winter traction and dry handling.

Figure 9 depicts the combined DMA performance, which attributed to radar plots and facilitated easy comparison to the tire tread applications. However, in tire tread applications, the criteria of silica-filled compounds make it difficult to find an optimum balance of better rolling resistance and good traction properties; this depends on the specific requirements. The experimental results indicate that the tanδ values of the 2Go and 1Go compound offered better performance in the rolling resistance. Silica with a higher surface area was desirable for achieving a lower rolling resistance and ice traction. It was achieved with proper reinforcement and without the addition of TESPT.

Morphology of the Composite

Figures 10 and 11 display the TEM images of the silica-filled compounds at a scale bar of 100 nm to demonstrate the silica dispersion in the composites. The dark phase represents silica dispersion.[35] The 2Go, 2G, 1Go, and 1G compounds delivered better dispersed silica particles, as shown by the TEM images. These results provide strong evidence that the physicomechanical properties, $\Delta E'$, and dynamic mechanical characteristics were

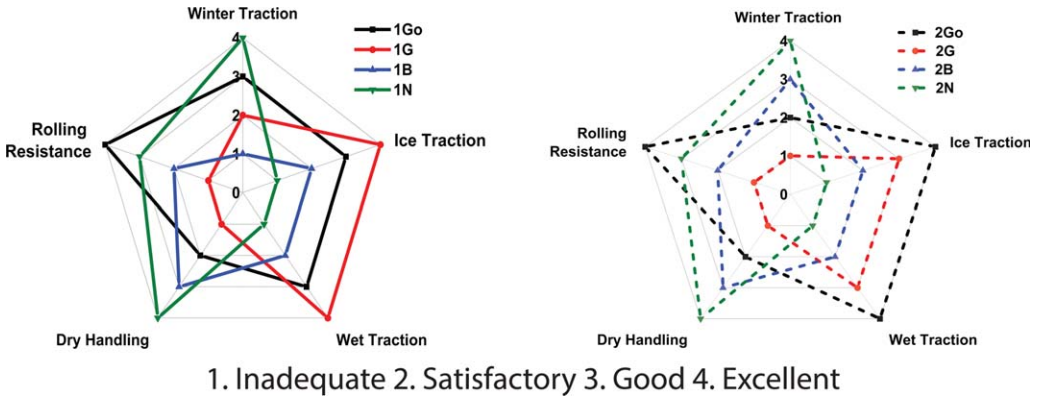

Figure 9. Radar plot for the combined DMA performance of the HD silica-filled rubber composites. [Color figure can be viewed in the online issue, which is available at wileyonlinelibrary.com.]

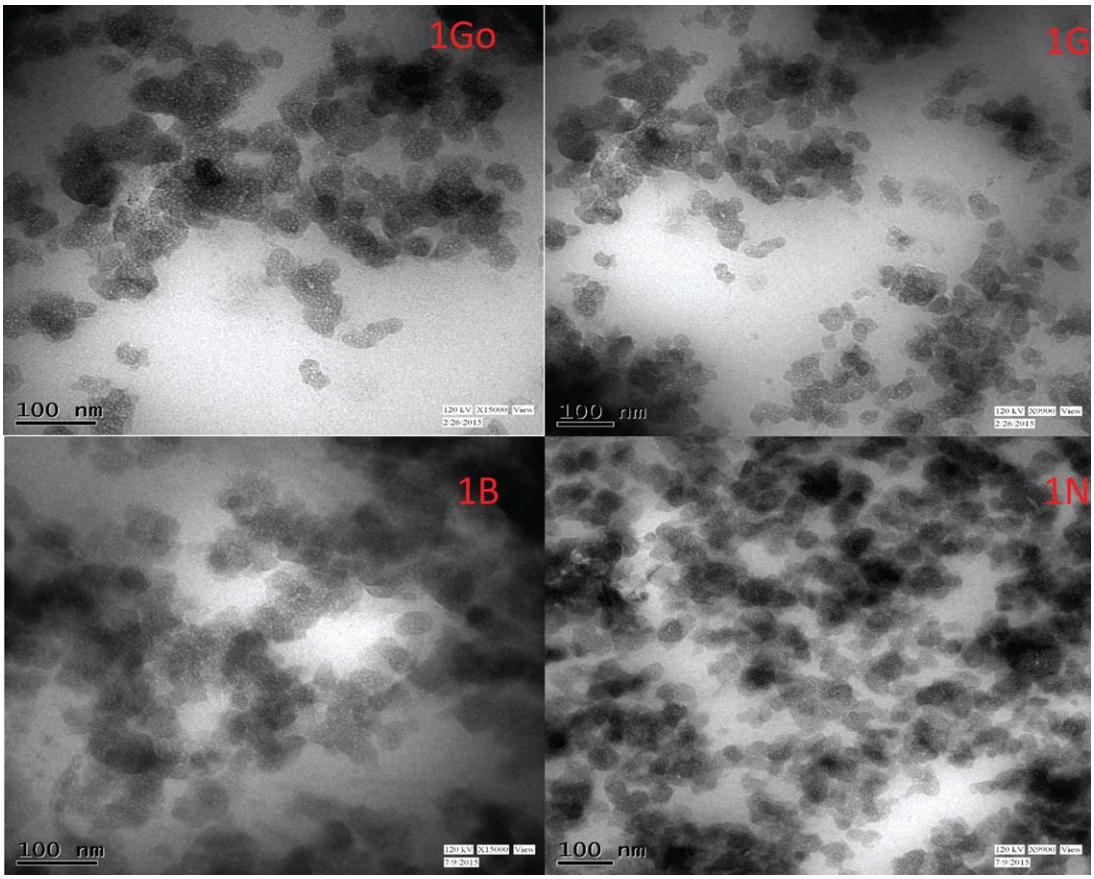

Figure 10. TEM images of the lower surface area HD silica-filled rubber composites (scale bar = 100 nm). [Color figure can be viewed in the online issue, which is available at wileyonlinelibrary.com.]

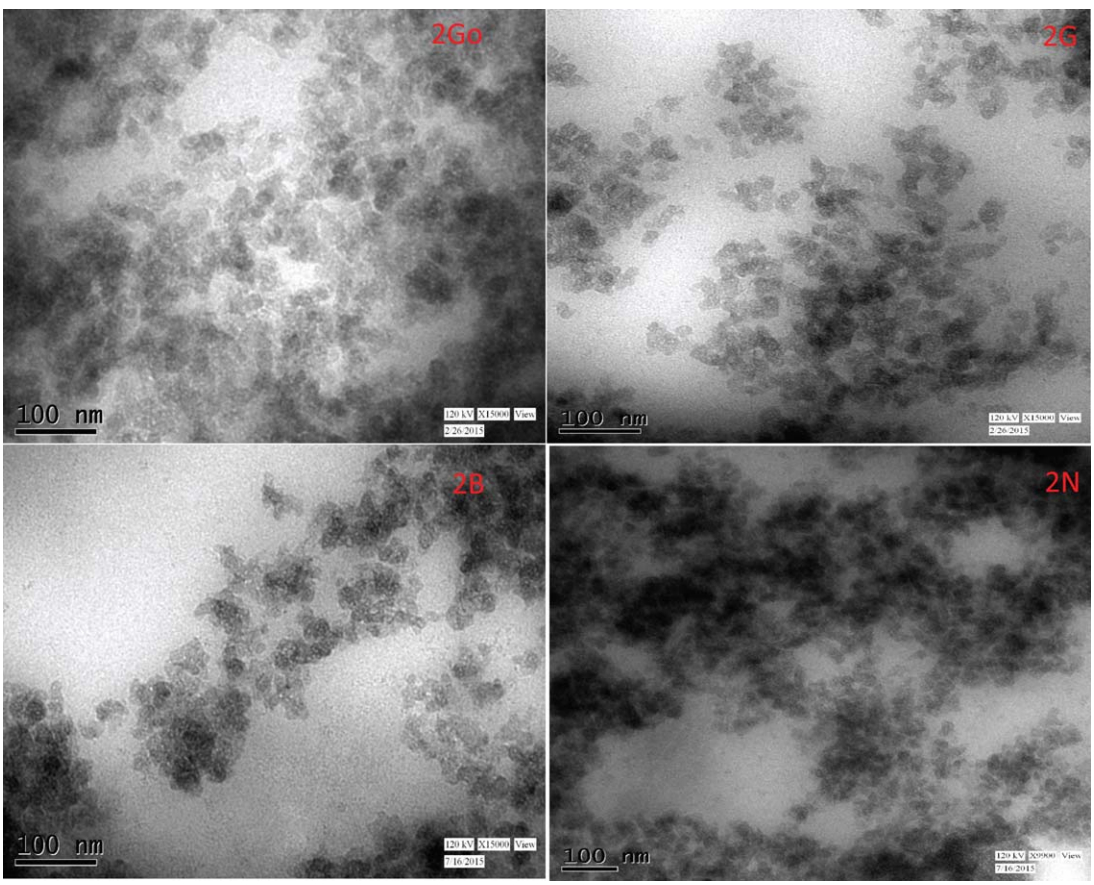

Figure 11. TEM images of the higher surface area HD silica-filled rubber composites (scale bar = 100 nm). [Color figure can be viewed in the online issue, which is available at wileyonlinelibrary.com.]

improved in the absence of TESPT. As expected, the high-surface-area-silica-particle dispersion was greatly improved in the ENR composites because of the strong attachment of the rubber network. The formation of hydrogen bonding with silanol groups helped to reduce voids in the compounds. Therefore, we concluded that the ENR 25 with high-surface-area silica helped to decrease the filler flocculation and led to superior dispersion in the silica compounds.

CONCLUSIONS

A successful attempt was made to mix silica of different surface areas in ENR 25 and NR composites with a melt-mixing method. The objective of this study was to examine the influence of the silica particle size in the magic triangle properties of the tire. We found that the incorporation of HD silica filler in ENR 25 and NR improved the physicomechanical and dynamic mechanical properties. HD silica with a high surface area in the absence of coupling agents delivered excellent properties, and the superior level of reinforcement in the composites was demonstrated by $\Delta E'$, BRC, and TEM observation. ENR with the high-surface-area silica composite exhibited an increased silica dispersion because of the epoxide functionality on NR. However, tanδ at 60 °C was significantly reduced in the higher silica-filled composites. In this study, we validated the potential of using ENR 25 in HD silica-based high-performance green tire tread composites and revealed that the application of these technologies can improve the fuel efficiency by lowering the rolling resistance of the tire tread.

ACKNOWLEDGMENTS

The authors are grateful to Vikas Rane (business director of Evonik), Mukesh Malhotra (director of Solvay Silica), Vikram R. Singh and Logesh (Apollo Tyres, the Netherlands), and Yezdi Patel (chief executive officer of Bymer Elastomers) for their assistance with the experiments and for stimulating discussions. Thanks are also given for the financial support of the Science and Engineering Research Board (New Delhi, India).

REFERENCES

1. Wolff, S.; Gorl, U.; Wang, M.; Wolff, W. *Eur. Rubber J.* **1994**, *176*, 16.
2. Byers, J. T. *Rubber Chem. Technol.* **2002**, *75*, 527.
3. Kaewsakul, W.; Sahakaro, K.; Dierkes, W. K.; Noordermeer, J. W. *J. Elastomers Plast.* **2015**, 56.
4. Manna, A. K.; De, P.; Tripathy, D. *J. Appl. Polym. Sci.* **2002**, *84*, 2171.
5. Dierkes, W. K. Ph.D. Thesis, University of Twente, **2005**.
6. Goerl, U.; Hunsche, A.; Mueller, A.; Koban, H. *Rubber Chem. Technol.* **1997**, *70*, 608.
7. Gelling, I. *J. Nat. Rubber Res.* **1991**, *6*, 184.
8. Ng, S.-C.; Gan, L.-H. *Eur. Polym. J.* **1981**, *17*, 1073.
9. Bandyopadhyay, A.; De Sarkar, M.; Bhowmick, A. *J. Mater. Sci.* **2005**, *40*, 53.
10. Noriman, N. Z.; Ismail, H. *J. Appl. Polym. Sci.* **2012**, *123*, 779.
11. Poh, B.; Tang, W. *J. Appl. Polym. Sci.* **1995**, *55*, 537.
12. Maiti, S.; De, S.; Bhowmick, A. K. *Rubber Chem. Technol.* **1992**, *65*, 293.
13. Chapman, A. V. In 24th International H. F. Mark-Symposium, Advances in the Field of Elastomers & Thermoplastic Elastomers, Vienna, **2007**; p 8.
14. Medalia, A. I. *Rubber Chem. Technol.* **1974**, *47*, 411.
15. Xu, H.; Liu, J.; Fang, L.; Wu, C. *J. Macromol. Sci. Phys.* **2007**, *46*, 693.
16. George, K. M.; Varkey, J. K.; Thomas, K.; Mathew, N. *J. Appl. Polym. Sci.* **2002**, *85*, 292.
17. Sankaran, K.; Nando, G. B.; Ramachandran, P.; Nair, S.; Govindan, U.; Arayambath, S.; Chattopadhyay, S. *RSC Adv.* **2015**, *5*, 87864.
18. Mihara, S. Ph.D. Thesis, University of Twente, **2009**.
19. Cook, S.; Chapman, A.; Tinker, A.; Oleksik, L. In Fall 172th ACS Rubber Division Meeting, Cleveland, OH, **2007**; p 16.
20. Kumar, S.; Chattopadhyay, S.; Sreejesh, A.; Nair, S.; Unnikrishnan, G.; Nando, G. *Mater. Res. Express* **2015**, *2*, 025001.
21. Saramolee, P.; Sahakaro, K.; Lopattananon, N.; Dierkes, W. K.; Noordermeer, J. W. *J. Elastomers Plast.* **2015**, 1.
22. Kaewsakul, W.; Sahakaro, K.; Dierkes, W.; Noordermeer, J. *Rubber Chem. Technol.* **2012**, *85*, 277.
23. Gheller, J.; Ellwanger, M. V.; Oliveira, V. *J. Elastomers Plast.* **2015**, 1.
24. Cataldo, F. *Macromol. Mater. Eng.* **2002**, *287*, 348.
25. Cichomski, E.; Tolpekina, T.; Schultz, S.; Dierkes, W. K.; Blume, A. In 11th Fall Rubber Colloquium, Hannover, Germany, **2014**; p 1.
26. Sarkawi, S. S.; Dierkes, W. K.; Noordermeer, J. W. *Rubber Chem. Technol.* **2013**, *88*.
27. Martin, P. J.; Brown, P.; Chapman, A. V.; Cook, S. *Rubber Chem. Technol.* **2015**, 88.
28. Guy, L.; Daudey, S.; Cochet, P.; Bomal, Y. *Kautsch. Gummi Kunst.* **2009**, *62*, 383.
29. Poh, B.; Ismail, H.; Quah, E.; Chin, P. *J. Appl. Polym. Sci.* **2001**, *81*, 47.
30. Kaewsakul, W.; Sahakaro, K.; Dierkes, W. K.; Noordermeer, J. W. *Polym. Eng. Sci.* **2015**, *55*, 836.
31. Rauline, R. (to Ets Michelin). European Pat. EP 0501 227 A1 (**1992**).
32. Kaewsakul, W.; Sahakaro, K.; Dierkes, W.; Noordermeer, J. *Rubber Chem. Technol.* **2014**, *87*, 291.
33. Sarkawi, S.; Dierkes, W.; Noordermeer, J. *Eur. Polym. J.* **2014**, *54*, 118.
34. Bao, Z.; Flanigan, C.; Beyer, L.; Tao, J. *J. Appl. Polym. Sci.* **2015**, 132.
35. Seo, B.; Kim, H.; Paik, H.-J.; Kwag, G.-H.; Kim, W. *Macromol. Res.* **2013**, *21*, 738.